Journal of Vibration Engineering & Technologies
https://doi.org/10.1007/s42417-022-00684-9

ORIGINAL PAPER

Damped Chatter Resistant Boring Bar Integrated with an Absorber Working in Conjunction with an Eddy Current Damper

Arjun Patel[1] · Ajay Yadav[1] · Mohit Law[1] · Bishakh Bhattacharya[2] · Pankaj Wahi[2]

Received: 8 June 2022 / Revised: 19 August 2022 / Accepted: 24 August 2022

Abstract

Purpose Slender boring bars vibrate when excited by cutting forces to result in chatter. These chatter vibrations damage the part and the tool and hence must be avoided and/or suppressed. Usually, tuned absorbers integrated within the boring bar dissipate the motion of the boring bar and make stable cutting possible. However, since the boring bar's dynamics change with loading and boundary conditions, optimally tuning the absorber becomes difficult. This prevents stable high-performance cutting. To improve the cutting performance of a potentially detuned absorber within a boring bar, this paper presents a novel hybrid damping solution. The hybrid damper is composed of an absorber working in conjunction with an eddy current damper.

Methods To demonstrate the working of this hybrid damper, we model the boring bar as an Euler–Bernoulli beam. A permanent magnet is supported by a spring and damper within a copper section of a boring bar. The supported magnet acts as an absorber and the relative motion between the conductive copper bar and the magnetic field induces eddy currents that hinder the motion of the boring bar. Governing equations for the beam with an integrated damper are obtained by applying the extended Hamilton's principle. Eddy current damping is evaluated by applying the Lorentz force law and the Biot–Savart law.

Results Our analysis suggests that the improvement in the chatter-free depth of cut with a hybrid damper over the case with a detuned absorber is as much as ~ 500%. And, when the absorber is optimally tuned and the hybrid damper takes its maximum possible value, the chatter-free depth of cut for both cases was found to be the same, suggesting that if/when the absorber can be optimally tuned, the eddy current damper offers no additional benefit.

Conclusion Since optimally tuning an absorber is difficult, our proposed hybrid damper offers a feasible solution to improve cutting performance with slender boring bars. Moreover, since our models are generalized, the approach may also be used to explore the integration of such hybrid dampers within other tooling systems such as milling tool holders.

Keywords Boring bar · Chatter · Detuned vibration absorber · Eddy current damper · Magnet · Vibration control

Introduction

Slender boring bars are flexible and hence susceptible to unstable chatter vibrations. These vibrations degrade machined surface quality, accelerate tool wear, and damage the tool. Since deep hole boring using slender tools has many important technological applications, suppressing chatter vibrations in boring has received sustained research attention. Efforts have centered on developing boring tools with materials having high stiffness and/or damping, on the use of passive dynamic vibration absorbers of the tuned mass kind, the use of particle and impact dampers, and the use of active vibration damping techniques. A nice overview of these is summarized in the seminal review paper on methods of chatter suppression [1]. Of these varied methods for improving damping, vibration absorbers are usually preferred due to their simple working principle, their relative ease of implementation, their not requiring external energy sources, and their low costs.

Vibration absorbers are typically characterized as a mass-spring-damper system attached to a primary system that they are to dissipate energy from. Their performance is governed

✉ Mohit Law
mlaw@iitk.ac.in

[1] Machine Tool Dynamics Laboratory, Department of Mechanical Engineering, Indian Institute of Technology Kanpur, Kanpur 208016, India

[2] Department of Mechanical Engineering, Indian Institute of Technology Kanpur, Kanpur 208016, India

Published online: 15 September 2022

by the ability to optimally tune the ratios of mass, frequency, and damping between the absorber and the primary system. Though there exist many methods to guide optimal tuning of the absorber [2–8] all methods presume the dynamics of the primary system to be fixed and unchanging. However, as research has shown, the dynamics of cantilevered tools such as boring bars change with loading, speed, and with boundary conditions [9–13]. Furthermore, the elastomeric mounts that support the absorber mass and provide the necessary stiffness and damping usually exhibit nonlinear characteristics and make optimal tuning difficult [9, 14]. Changing dynamics of the primary system and difficulties in optimally tuning the absorber may result in a detuned system, i.e., a system in which the absorber is not optimally tuned. This may in turn degrade the performance of the absorber and compromise its ability to suppress chatter vibrations.

To address the need to suppress chatter vibrations with a boring bar integrated with a potentially detuned vibration absorber, this paper proposes the use of an eddy current damper to work in conjunction with the absorber. Eddy current dampers are contactless and do not modify the primary system and can be easily integrated within a boring bar by simply replacing the absorber mass with a permanent magnet. The eddy current thus induced due to the relative motion between the conducting boring bar and the magnetic field will produce resistive viscous forces that will help dissipate energy. Characterizing the workings of such a novel hybrid damper is the focus and main contribution of this paper.

Though the use of eddy currents in our proposed manner is new, because of the advantages they offer, eddy currents have found use in several other dynamical systems such as in brakes, for suppression of rotor vibrations, and in isolation of structural vibrations [15, 16]. Eddy current damping has also been used to successfully suppress beam vibrations [17–20]. In the context of machine tool systems, eddy current dampers have been used to suppress chatter vibrations in the milling of thin-walled parts [21], to suppress spindle vibrations in a robotic milling process [22], to develop non-contacting fixtures for chatter-free machining of cantilevered workpieces [23], and to design a tunable clamping table to avoid chatter in milling [24].

Though absorbers and eddy current dampers have proved effective when used in their individual capacities, there are studies reporting the advantage of using both together [25–31]. In some exemplary work, improvements in damping of cantilevered systems were reported with a permanent magnet as the concentrated mass of the absorber [25–27]. Separately, the performance of an eddy current–tuned mass damper combined for different permanent magnet topologies was reported in [28]. Other work also demonstrated an adaptive tuned mass damper based on shape memory alloys and eddy currents [29]. And, yet other work demonstrated the effectiveness of an eddy current tuned mass damper to damp vibrations of an offshore wind turbine [30] and a long gun barrel [31].

Though previous studies on eddy current dampers and absorbers combined with eddy current damping have guiding significance for the present work, in all previous work, the magnet was placed outside the artefact to be damped, and hence those findings are not directly relevant to our application of interest in which any magnet must be integrated within the boring bar, and not outside of it such as to not reduce the boring bar's effective working length. Since the magnet must be placed inside of the boring bar, it must be supported in mounts. And since it must be supported in mounts that have a finite stiffness and damping, and since the magnet has mass, it also acts as a vibration absorber. And, since the magnet moves relative to the boring bar, it also induces eddy currents that resist the motion of the boring bar. This combination of the magnet as an absorber and one that induces eddy current damping is a new concept and is the main novelty of the paper. Model-based analysis of this new concept is the main new technical contribution of this paper.

Moreover, in most previous research on damped tooling systems, the primary system to be damped was almost always modelled as a single degree of freedom system. While that approximation may have been reasonable for those systems of interest, modelling the boring bar as a single degree of freedom system presumes attachment of the damper at the free end of the cantilevered tool, which is also the cutting end, and hence any design solution may not necessarily be feasible and/or practically realizable.

To realize a design of a boring bar integrated with a hybrid damper, i.e., an absorber working in conjunction with an eddy current damper, we present systematic model-based parametric investigations. A schematic of a possible design is shown in Fig. 1.

The boring bar is cantilevered. The free end supports the cutting cartridge. The cartridge is mounted on an end-plug which is solid and made of copper. That section is connected to another copper section that is partly hollow. The cavity within that section accommodates the damping artifacts. If the boring bar is to be used with only an absorber, the damping artefact will consist of the absorber mass supported in two O-rings that provide the necessary stiffness and damping. There is a slider and a tuner to tune the absorber as necessary. If the bar is to be used with a hybrid damper, a permanent magnet can replace the absorber mass, as necessary. The partly hollow section is screw mounted on another section that is solid and made of steel. Copper is preferred due to its conductivity being high. And, to ensure that eddy currents that are generated due to the relative motion of the magnet do not leak across the interfaces, the end plug is also made of copper.

Since the absorber/magnet is placed away from the cutting end and since it is of interest to damp the response at the free end to enable chatter-free machining, classical

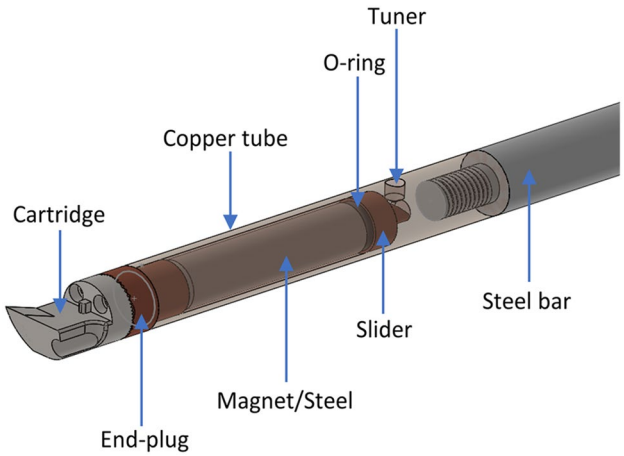

Fig. 1 Schematic of a damped boring bar integrated with a hybrid passive damper

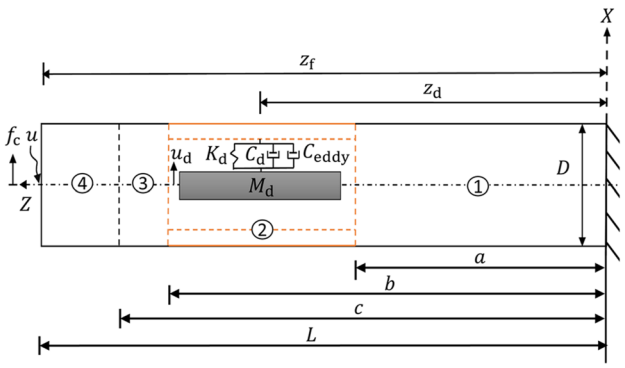

Fig. 2 Schematic of a boring bar modelled as an equivalent cantilever beam integrated with a hybrid passive damper

model-based methods [2–4] to tune the absorber that presumes it is located at the free end are not suitable. This aspect is addressed herein by modelling the boring bar as a damped cantilevered Euler–Bernoulli beam, which, as has been reported elsewhere too, is the appropriate method to model slender tooling systems [6–10]. The absorber is modelled as a point mass-spring-damper system placed anywhere along the beam. This model and the model for eddy current damping effects are detailed in the 'Modeling' section of the paper. All analysis presented herein is for the case of a stationary boring bar with a rotating workpiece.

Since the magnet must be incorporated inside of the boring bar, there is hence a complex interaction between the dynamics of the primary boring bar system, the eddy current damping effect, and the magnet as an absorber. The parametric analysis presented in this paper characterizes these complex interactions. Such analysis is new and has not been reported on in the published literature. Since an experimental route to characterize these complex interactions would require many prototypes to be built, with which we would have to adopt a try-and-see approach, and since such a strategy would be time-consuming and cost-prohibitive, we prefer the model-based approach in this paper. The model-based analysis is expected to instruct prototype development, which can be tested in future works.

Model-based parametric investigations are presented in the section titled 'Evaluating eddy current damping and tuning the absorber'. We characterize the role of the eddy current damper and the absorber. To tune the absorber/magnet placed away from the cutting end, we maximize the chatter-free stability limit, which we treat as the objective function in a numerical scheme based on the minimax method [8]. We also present a comparative analysis of the proposed hybrid damper with that of a solid boring bar and with that of a boring bar integrated with a (sub)optimally tuned absorber. That analysis is presented in a section titled 'Comparative analysis with the hybrid damper'. That analysis is followed by conclusions.

Dynamical Model of the Boring Bar Integrated with a Hybrid Damper

The governing equations of motion of the boring bar integrated with a hybrid damper are derived herein using the extended Hamilton's principle, followed by a discussion on methods to solve for the free and forced vibration response. The slender boring bar of length L and diameter D is modelled as a clamped-free damped Euler–Bernoulli beam. Since the bar is stiff along its axis, and since only the flexibility in the radial direction influences its machining stability [32], only the radial direction (X direction) flexibility is considered.

A schematic of the model of the boring bar is shown in Fig. 2. The model follows the design shown in Fig. 1. The four sections of interest are highlighted in Fig. 2. The first section extends up until a distance a from the fixed end. In this section, the bar is solid, and the material is steel. The second section is hollow and made of copper. It starts at a, and extends up to b from the clamped end. The magnet/absorber of mass M_d is assumed lumped and attached at a distance z_d from the fixed end within this section. Though the mass is supported in two O-rings, the model approximates them with an equivalent stiffness K_d and damping C_d, respectively. And, though the mass is attached along the beam's axis in the model, the schematic shows it attached to the inner diameter of the beam. The third section is solid and made of copper and the fourth section is also solid but made of steel.

The eddy current damping force acting on the beam is also assumed to be acting at a distance z_d from the clamped end. Since the eddy current damping effect is modelled to be superposed with the absorber, both damping effects are shown to be in parallel in the schematic in Fig. 2.

Assuming the deflection of the beam as 'u' along the radial direction, the kinetic and the potential energy of the beam can be defined as [33]:

$$T_{beam} = \frac{1}{2}\int_0^L \rho A\left(\frac{\partial u}{\partial t}\right)^2 dz, \tag{1}$$

$$U_{beam} = \frac{1}{2}\int_0^L EI\left(\frac{\partial^2 u}{\partial z^2}\right)^2 dz, \tag{2}$$

where in ρ is the density of the beam, A is the cross-sectional area, u is the displacement of the beam, E is the modulus of elasticity, I is the area moment of inertia, and EI represents the bending rigidity. E, I, A, ρ are function of the section of interest, i.e., of z.

Since the beam is damped, the work done by the internal damping (ID) force, f_{ID} on the beam can be written as:

$$W_{ID,beam} = \int_0^L f_{ID} u\, dz. \tag{3}$$

Since the absorber will also damp beam motion, the damping forces of the absorber, f_D on the beam can be written as:

$$W_{D,beam} = \int_0^L f_D u\, \delta(z - z_d) dz, \tag{4}$$

where in δ is the Dirac delta function.

Moreover, since the magnet moving inside a copper cylinder will generate an eddy current damping force, the work done by the force, $W_{e,beam}$ on the beam can be written as:

$$W_{e,beam} = \int_0^L f_e u\, \delta(z - z_d) dz, \tag{5}$$

where in f_e is the eddy current damping force on the beam and is obtained as described in the next subsection.

Furthermore, since the force generated during the machining process will also act on the tool, the external work done by this cutting force, f_c on the beam can be written as:

$$W_{c,beam} = \int_0^L f_c u\, \delta(z - z_f)\, dz, \tag{6}$$

where in z_f represents the location of the cutting insert from the clamped end.

As above, the kinetic and potential energies of the dynamic vibration absorber (DVA) can be similarly defined as:

$$T_{DVA} = \frac{1}{2}\int_0^L M_d\left(\frac{\partial u_d}{\partial t}\right)^2 \delta(z - z_d)\, dz, \tag{7}$$

$$U_{DVA} = \frac{1}{2}\int_0^L K_d u_d^2\, \delta(z - z_d)\, dz, \tag{8}$$

where in u_d is the displacement of the absorber in the radial direction.

Work done on the absorber by the damping force, $f_{D,DVA}$ of the absorber can be written as:

$$W_{D,DVA} = \int_0^L f_{D,DVA} u_d\, \delta(z - z_d)\, dz, \tag{9}$$

and, the work done by the eddy current damping force, $f_{e,DVA}$ on the absorber can be written as:

$$W_{e,DVA} = \int_0^L f_{e,DVA}\, u_d\, \delta(z - z_d) dz. \tag{10}$$

Using definitions of energies of the beam and the absorber, and considering the work done in the system, the generalized extended Hamilton's principle can be applied as [33]:

$$\begin{aligned}\delta_v \int_{t_1}^{t_2} \big(&T_{beam} + W_{ID,beam} + W_{D,beam} + W_{e,beam} \\ &+ W_{c,beam} + W_{D,DVA} + W_{e,DVA} + T_{DVA} \\ &- U_{beam} - U_{DVA}\big) dt = 0,\end{aligned} \tag{11}$$

where in δ_v is the variational operator, and t_1 and t_2 are the time intervals in the dynamic trajectory.

Substituting the energies of the beam and the absorber and the work done on each from Eqs. (1–10) into Eq. (11), and assuming that the beam's damping can be represented with a coefficient C_b, and that the absorber's is C_d, and that C_{eddy} is the eddy current damping coefficient, and further assuming that the damping forces can take the form of $f_{ID} = -\frac{C_b}{L}\left(\frac{\partial u}{\partial t}\right)$; $f_D = -f_{D,DVA} = -C_d\left(\frac{\partial u}{\partial t} - \frac{\partial u_d}{\partial t}\right)$; $f_e = -f_{e,DVA} = -C_{eddy}\left(\frac{\partial u}{\partial t} - \frac{\partial u_d}{\partial t}\right)$, the resulting governing differential equation of motion of the beam and the absorber can be simplified and shown to be:

$$\begin{aligned}&\rho A\frac{\partial^2 u}{\partial t^2} + \frac{C_b}{L}\frac{\partial u}{\partial t} + EI\frac{\partial^4 u}{\partial z^4} + \left[C_d\left(\frac{\partial u}{\partial t} - \frac{\partial u_d}{\partial t}\right) + K_d(u - u_d)\right] \\ &\delta(z - z_d) + C_{eddy}\left(\frac{\partial u}{\partial t} - \frac{\partial u_d}{\partial t}\right)\delta(z - z_d) = f_c(z,t)\delta(z - z_f),\end{aligned} \tag{12}$$

$$\left[M_d\frac{\partial^2 u_d}{\partial t^2}+C_d\left(\frac{\partial u_d}{\partial t}-\frac{\partial u}{\partial t}\right)\right.$$
$$\left.+K_d\left(u_d-u\right)+C_{eddy}\left(\frac{\partial u_d}{\partial t}-\frac{\partial u}{\partial t}\right)\right]\delta\left(z-z_d\right)=0. \tag{13}$$

If the response of the beam with only an absorber was of interest, C_{eddy} could be neglected in the above equations. If, however, the influence of eddy current damping was also of interest, C_{eddy} should be evaluated as described next.

Evaluating the Eddy Current Damping

We evaluate the eddy current damping for a magnet that has a length L_m and radius R_m and that is placed inside the hollow cavity within Sect. 2 of the boring bar–see Figs. 1 and 2. The copper cavity has an inner radius of r_c and an outer radius of R_c. Its length L_c is assumed the same as the magnet for purposes of evaluation of the eddy current damping.

When the boring bar vibrates, the relative motion between the magnet and the conductor will induce a time-varying magnetic field that will generate eddy currents in the copper conductor. The magnetic field induced by these eddy currents generated in the conductor will be such that it will oppose the initial magnetic field induced due to the relative motion between the magnet and the conductor. Due to the generation of eddy currents and the resistance of the conductor, the mechanical energy due to vibration will likely dissipate through Joule heating in the conductor. Since the boring bar will vibrate when excited with cutting forces, the magnetic flux will keep changing and eddy currents will keep regenerating, thereby dissipating energy continuously.

The force generated due to eddy currents can be obtained from the Lorentz force law, and can be shown to be [18]:

$$f_e=\int_V J\times B\,dV \tag{14}$$

where in J is the induced total eddy current density, B is the magnetic flux density, and V is the volume of the conductor. The eddy currents induced in the conducting material depend on the cross product of the magnetic flux and the velocity, i.e., $J=\sigma(v\times B)$, wherein σ is the conductivity of the conductor.

Since the radial component of the magnetic field density is parallel to the velocity of the beam, it does not contribute to the generation of eddy currents, and only the axial component does. And, though eddy current generation is a complex multi-physics phenomenon, the magnetic flux density at any point in space due to the permanent magnet can be obtained analytically using the Biot-Savart law, and then this elemental analysis can be integrated for the whole length of the conductor. For the configuration shown in Fig. 3, the axial magnetic flux density at any point (r,z) can be shown to be [34]:

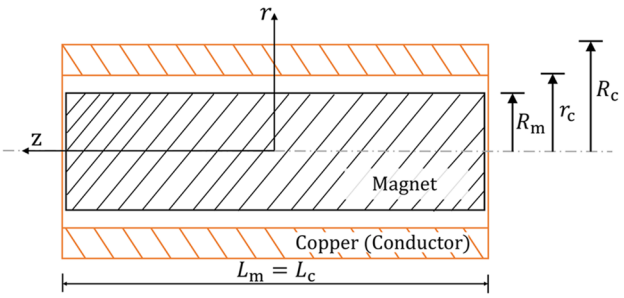

Fig. 3 Schematic representation of the permanent magnet within a copper tube

$$B_z=\frac{\mu_o M_o}{2\pi}\int_{-\frac{L_m}{2}}^{\frac{L_m}{2}}\frac{1}{\left[\left(R_m+r\right)^2+\left(z-z_1\right)^2\right]^{\frac{1}{2}}}$$
$$\left[\frac{R_m^2-r^2-\left(z-z_1\right)^2}{\left(R_m+r\right)^2+\left(z-z_1\right)^2}C(k)+D(k)\right]dz_1, \tag{15}$$

where in μ_o is the permeability of the free space, z_1 is the distance from the center of the magnet in the Z-direction, and M_o is the magnetization constant, and $C(k)$ and $D(k)$ are the elliptical integrals of the first and second kind, respectively [34]:

$$D(k)=\int_0^{\pi/2}\frac{1}{\sqrt{\left(1-k^2\theta\right)}}d\theta, \tag{16}$$

$$C(k)=\int_0^{\pi/2}\sqrt{1-k^2\theta}\,d\theta, \tag{17}$$

where in k is [34]:

$$k=\sqrt{\frac{4Rr}{\left(R_c+r\right)^2+\left(z-z_1\right)^2}} \tag{18}$$

From Eqs. (14)–(18), the damping force on the beam can be shown to become:

$$f_e=-2\sigma\pi v\int_{-\frac{L_c}{2}}^{\frac{L_c}{2}}\int_{r_c}^{R_c}rB_z^2\,dr\,dz. \tag{19}$$

The eddy current damping force is evaluated by using the Gauss-Quadrature method to numerically solve the elliptical integrals. The direction of the force opposes the direction of the velocity of the beam and can be explained from Eq. (14) and

from Fig. 3–in which the direction of the velocity of the beam is considered along the X-direction (magnet's radial direction), and the axial component of the magnetic flux density is along the Z-direction. Considering $\hat{i}$, $\hat{j}$, and $\hat{k}$ to be the unit vectors along the X, Y, and Z directions, respectively, the direction of the damping force would be $\left(\hat{i}\times\hat{k}\right)\times\hat{k}=-\hat{i}$, i.e., it would be opposite to the direction of the velocity of the beam.

Equation (19) can be re-written as:

$$f_e=-\left(C_{eddy}\,v\right), \tag{20}$$

where in C_{eddy} is the eddy current damping coefficient to be used in Eqs. (12)–(13). From Eq. (15) it is evident that C_{eddy} is a function of the magnet's geometry (L_m, R_m) and its grade (M_o), and of the gap in between the magnet and the conductor (r_c-R_m), as well as of the thickness (R_c-r_c) and material of the conductor (σ).

Solving the Governing Equations of Motion

To solve the governing differential equations of motion for a beam integrated with a hybrid damper, we assume the modal solution of the beam can be written as:

$$u(z,t)=\sum_r \phi_{\gamma r}(z)q_r(t), \tag{21}$$

where in q_r represents the time component of the displacement of the beam at any location 'z', $\phi_{\gamma r}$ are the mode shapes of the beam, 'γ' depends on the section of the beam considered i.e., 1, 2, 3, or 4, and 'r' represents the mode number. The mode shapes that depend on the section of the beam in consideration can be written as [33]:

$$\phi_\gamma=B_{1\gamma}\cos\left(\beta_\gamma z\right)+B_{2\gamma}\cosh\left(\beta_\gamma z\right)+B_{3\gamma}\sin\left(\beta_\gamma z\right)+B_{4\gamma}\sinh\left(\beta_\gamma z\right)$$
$$\gamma=\begin{cases}1, & 0\le z\le a\\ 2, & a<z\le b\\ 3, & b<z\le c\\ 4, & c<z\le L\end{cases} \tag{22}$$

The natural frequency of the beam, irrespective of the sections will remain 'ω' and can be expressed in terms of β and the geometrical parameters of each section as:

$$\omega=\beta_1^2\sqrt{\frac{E_1I_1}{\rho_1A_1}}=\beta_2^2\sqrt{\frac{E_2I_2}{\rho_2A_2}}=\beta_3^2\sqrt{\frac{E_3I_3}{\rho_3A_3}}=\beta_4^2\sqrt{\frac{E_4I_4}{\rho_4A_4}}. \tag{23}$$

Sections 1 and 4 are made of steel and have different cross-sectional geometries. Likewise, Sects. 2 and 3 are made of copper and have different cross-sectional geometries. Hence, the relationship between β_1, β_2, β_3 and β_4 can be re-written as:

$$\beta_4=\beta_1\left[\frac{E_1I_1\rho_4A_4}{E_4I_4\rho_1A_1}\right]^{\frac{1}{4}}=\beta_2\left[\frac{E_2I_2\rho_4A_4}{E_4I_4\rho_2A_2}\right]^{\frac{1}{4}}=\beta_3\left[\frac{E_3I_3\rho_4A_4}{E_4I_4\rho_3A_3}\right]^{\frac{1}{4}} \tag{24}$$

The appropriate boundary conditions at the clamped end are:

$$\phi_1(0)=0;\quad \phi_1'(0)=0, \tag{25}$$

i.e., the slope and deflection are zero, and, at the free end, the shear force and the bending moment are zero:

$$E_4I_4\phi_4''(L)=0;\ E_4I_4\phi_4'''(L)=0. \tag{26}$$

Since the model of the boring bar assumes four sections, to ensure continuity, the compatibility conditions such as the deflection, slope, shear force, and the bending moment at the interface $z=a$ from the fixed end are:

$$\begin{aligned}&\phi_1(a^-)=\phi_2(a^+);\qquad \phi_1'(a^-)=\phi_2'(a^+);\\ &E_1I_1\phi_1''(a^-)=E_2I_2\phi_2''(a^+);\qquad E_1I_1\phi_1'''(a^-)=E_2I_2\phi_1'''(a^+).\end{aligned} \tag{27}$$

Similarly, the compatibility conditions at the interface $z=b$ from the fixed end are:

$$\begin{aligned}&\phi_2(b^-)=\phi_3(b^+);\qquad \phi_2'(b^-)=\phi_3'(b^+);\\ &E_2I_2\phi_2''(b^-)=E_3I_3\phi_3''(b^+);\qquad E_2I_2\phi_2'''(b^-)=E_3I_3\phi_3'''(b^+),\end{aligned} \tag{28}$$

and the compatibility conditions at the interface $z=c$ from the fixed end are:

$$\begin{aligned}&\phi_3(c^-)=\phi_4(c^+);\qquad \phi_3'(c^-)=\phi_4'(c^+);\\ &E_3I_3\phi_3''(c^-)=E_4I_4\phi_4''(c^+);\qquad E_3I_3\phi_3'''(c^-)=E_4I_4\phi_4'''(c^+),\end{aligned} \tag{29}$$

where in the superscripts '$-$' and '$+$' denote the positions slightly before and slightly after the interfacial point(s), respectively, and '', ''', and '''' denote the first, second, and third derivatives with respect to z.

The four boundary conditions in Eq. (25) and in Eq. (26) and the twelve compatibility conditions in Eqs. (27, 28, 29) are used to solve the sixteen unknowns in the mode shape expression in Eq. (22). The solution to these will result in equations in β, which then can be solved to find the natural frequency of the beam, and in turn the mode shapes. The obtained mode shapes are substituted in the assumed solution in Eq. (21), and the assumed solution is in turn substituted in the governing equations of motion of the beam and absorber in Eq. (12) and Eq. (13).

Multiplying the updated Eq. (12) and Eq. (13) with mode shape $\phi_{\gamma s}$, where s is mode number and integrating from zero to the length of the beam, and by using the property of orthogonality of the mode shapes, Eq. (12) and Eq. (13) are transformed as:

$$\ddot{q}_s\left(\int_0^L \rho_\gamma A_\gamma \phi_{\gamma s} d_z\right) + \dot{q}_s\left(\frac{C_b}{L}\int_0^L \phi_{\gamma s}\phi_{\gamma s} dz\right) + q_s\left(E_\gamma I_\gamma \beta_\gamma^4 \int_0^L \phi_{\gamma s}\phi_{\gamma s} dz\right) + \left[C_d\left(\sum_r \dot{q}_r\phi_{\gamma r} - \dot{u}_d\right)\phi_{\gamma s} + K_d\left(\sum_r q_r\phi_{\gamma r} - u_d\right)\phi_{\gamma s} + C_{eddy}\left(\sum_r \dot{q}_r\phi_{\gamma r} - \dot{u}_d\right)\phi_{\gamma s}\right]\delta(z - z_d) = f_c(z_f, t)\phi_{\gamma s}, \tag{30}$$

$$M_d\ddot{u}_d + \left[K_d\left(u_d - \sum_r \phi_{\gamma r} q_r\right) + \left(C_d + C_{eddy}\right)\left(\dot{u}_d - \sum_r \phi_{\gamma r}\dot{q}_r\right)\right]\delta(z - z_d) = 0. \tag{31}$$

These equations, i.e., Eq. (30) and Eq. (31) represent the equations of motion of the beam and the absorber in the X direction, respectively, and 'r', 's' represents any two different modes of the beam. These equations can be written in a compact matrix form as:

$$[M]\{\ddot{q}\} + [C]\{\dot{q}\} + [K]\{q\} = \{f\}, \tag{32}$$

where in $\{q\} = \{q_s, u_d\}^T$, $\{f\} = \{f_c\phi_{\gamma s}(z_f), 0\}^T$, and $[M]$ represents the mass matrix, $[C]$ represents the damping matrix, and $[K]$ represents the stiffness matrix.

Since the free and forced vibration response are both of interest, and since forced vibration response is best characterized using frequency response functions (FRF), to obtain the FRFs, the excitation and the response is assumed to be harmonic, i.e., $f_c(t) = F_c e^{i\omega t}$, $q(t) = Qe^{i\omega t}$, and $u_d(t) = U_d e^{i\omega t}$. Thus, the frequency response function matrix $[H]$ becomes:

$$[H] = [R]\left[\frac{1}{(-\omega^2)[M] + (i\omega)[C] + [K]}\right][F] \tag{33}$$

$_{\text{w}}$here in $[R] = [\phi_\gamma(z_r)0;01]$ is the response matrix, and $[F] = [\phi_\gamma(z_f)0;00]$ represents the forcing matrix, wherein $\phi_\gamma(z_f)$ and $\phi_\gamma(z_r)$ are the eigenvectors at the excitation and response location, respectively.

Having detailed the analytical model for evaluating the dynamics of a boring bar integrated with a hybrid damper, parametric analysis for the eddy current damper and methods to tune the absorber are discussed next.

Evaluating Eddy Current Damping and Tuning the Absorber

Since the eddy current damping effect is a function of the geometry of the magnet and of the size of hollow copper cavity, and since the magnet is also an absorber, and since any change in its size and/or a change in the size of the hollow copper cavity will change the way in which the absorber must be tuned, both mechanisms of damping are linked. An optimal solution to the problem will likely require setting up a multi-variable optimization problem seeking to find a balance between the damping offered by the eddy current damper and by the absorber. However, since setting up such a multi-variable optimization problem is difficult, we instead size the eddy current damper based on model-based parametric investigations. Those discussions are first presented herein. We follow those discussions with separate discussions on the model-based tuning of an absorber.

All model-based analysis is presented for a representative case of the boring bar with a diameter of 25 mm and a length of 200 mm, i.e., for the case of the length to diameter ratio being 8. The bar has the same constructional features as shown in Fig. 1 to accommodate the hybrid damper. The solid section at the fixed end is assumed made of steel with a density of $\rho_1 = 7850\text{kg/m}^3$ and a modulus of elasticity of $E_1 = 200\text{GPa}$. The hollow section is made of copper with a density of $\rho_2 = 8960\text{kg/m}^3$ and a modulus of elasticity of $E_2 = 120\text{GPa}$. The end plug of length 28 mm is also made of copper with the same properties. The cartridge at the free end of length 30 mm that is made of steel is not prismatic, and is hence modelled to have an equivalent diameter of ~ 19 mm. The length and cross-sectional features of the second section are determined based on parametric analysis (discussed next) of the influence of the size of the absorber and the eddy current damper. The length of the solid section at the fixed end depends on the length of the hollow section and is adjusted accordingly such that the total length remains 200 mm.

The mode-dependent structural damping of the boring bar is assumed to be of the form $C_{b_s} = \frac{2\zeta_b M_s \omega_{ns}^2}{\omega}$, wherein M_s is the modal mass of the s^{th} natural frequency, ω is the excitation frequency, and ζ_b is assumed to be0.3%.

Eddy Current Damping

It is evident from Eq. (15) and Eq. (20) that the eddy current damping scales with the magnet's grade and with the material of the conductor—parameters that are constrained by the grade of the magnet that is commercially available and by the choice of the conductive material. On the other hand, dependence of C_{eddy} of the conductor's thickness, on the magnet's size, and on the gap in between the magnet and the conductor is less intuitive. Since the outer diameter of the boring bar is fixed to be 25 mm, and since a wall thickness of 2 mm is thought necessary for the boring bar

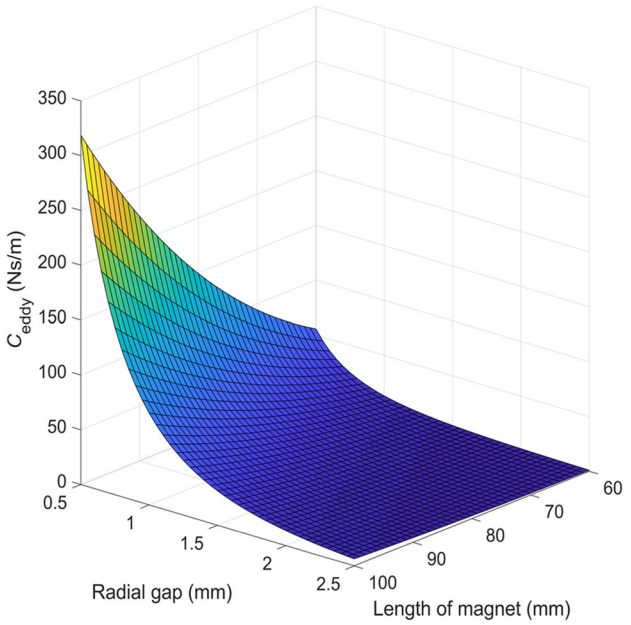

Fig. 4 Eddy current damping changes with the length of the magnet and with the gap in between the magnet and the conductor

to have sufficient strength against bending, we investigate herein only how C_{eddy} changes with the magnet's length and with the gap in between the magnet and the conductor.

These characteristics are shown in Fig. 4. A change in the length of the magnet is associated with a corresponding change in the length of the conductor (see Fig. 3), and a change in gap can be thought to be brought about by a change in the diameter of the magnet. Results in Fig. 4 assume the use of a neodymium magnet of the *N*52 grade that has a magnetization constant of $5.45 \times 10^5 A/m$ [35] placed inside a copper conductor with a conductivity of $5.8 \times 10^7 S/m$.

Analysis in Fig. 4 is limited to the range of 0.5 mm to 2.5 mm for the gap and to the range of 60 mm to 100 mm for the length. Since the magnet will also work as an absorber, and since absorbers vibrate with amplitudes larger than the primary system to dissipate energy, and since potential vibrations of the boring bar can be of the order of several hundred micrometers [5], gaps (between the magnet and the conductor) lower than 0.5 mm may result in infeasible design solutions. Similarly, since the overall length of the boring bar is 200 mm, of which some is taken up by the cutting cartridge at the free end and some by the solid section towards its fixed end, and since the magnet is housed in the hollow middle section, lengths of the magnet greater than 100 mm might also not result in feasible designs.

As is evident from Fig. 4, C_{eddy}, in general, reduces with an increase in the gap between the magnet and the conductor and increases with an increase in the length of the magnet. Though the dependence is nonlinear, results suggest that the gap should be as low as possible and the magnet should be also long as possible, i.e., if the size of interest is commercially available. Since magnets of 20 mm diameter and 80 mm lengths are available, the magnet's size is fixed as such. Fixing the size of the magnet also fixes its mass for its use as an absorber.

Tuning the Absorber

The absorber's performance is governed by its mass, stiffness, and damping, and the relationship of these parameters with those of the system being damped. Usually, these parameters are tuned using Den Hartog's [2] classical method that approximates the primary system as an undamped single degree of freedom system. This approximation presumes absorber placement at the free end. Since the absorber is placed away from the free end, we instead suggest tuning the absorber by maximizing the boring bar's chatter-free absolute minimum stable depth of cut.

To maximize the chatter-free depth of cut, we use the classical model that suggests that the limiting speed-independent depth of cut, b_{lim} is a function of the real part of the boring bar's FRF in the radial direction and of the radial cutting force coefficient [5]:

$$b_{\text{lim}} = -\frac{1}{2K_r \text{Re}[H]} \tag{34}$$

Since b_{lim} is governed by the dynamics characterized by the FRF, we set up an optimization problem to find the absorber's parameters (K_d, C_d) for a given mass (M_d) of the absorber that is fixed based on the already selected size of the magnet. The objective function to maximize the chatter-free depth of cut is:

$$\begin{aligned} &\text{maximize } f_{obj}\left(K_d, C_d\right) = \left(b_{\text{lim}}\right) \\ &\text{subject to}: \quad 1 \times 10^2 < K_d < 1 \times 10^7; 10 < C_d < 500 \end{aligned} \tag{35}$$

We maximize Eq. (35) using the Nelder–Mead optimization algorithm [36]. The search space for stiffness and damping is informed by reports in [8], and the initial guess for the stiffness and damping of the absorber are taken as 1×10^3 N/m and 100 N-s/m, respectively.

Having discussed the evaluation of eddy current damping, and the method of tuning the absorber, we next present a comparative analysis of the dynamics and chatter-free cutting capability of the proposed hybrid damper and compare its behavior with that of a solid boring bar without an absorber, and with that of a boring bar integrated with a (sub)optimally tuned absorber.

Comparative Analysis with the Hybrid Damper

Dynamics and chatter-free cutting capability of a boring bar with a hybrid damper, i.e., one in which an eddy current damper works in conjunction with an absorber is discussed herein. The performance of the hybrid damper is also contrasted herein with the case of the boring bar integrated with an absorber that may or not be optimally tuned by maximizing the chatter-free depth of cut. For maximizing the chatter-free depth of cut, we assume cutting of aluminum with a radial cutting force coefficient of 580 N/mm^2. These results are also contrasted with the dynamics and cutting capability of a solid boring bar without a damper integrated within it. All analysis herein is limited to discussing only the first fundamental bending and most flexible mode of the boring bar.

Analysis herein limits the comparisons to the case of an absorber placed at a length of 102 mm from the fixed end. The eddy current damping effect also acts at the same location. Constructional restrictions prohibit the placement of the absorber any closer to the free end. Since the absorber mass is to be subsequently replaced by a permanent magnet for the case of the hybrid damper, and since steel and the magnet made of neodymium have similar densities, we limit analysis herein only for the case of using an absorber made of steel, even though an absorber made of tungsten carbide might fare better [8]. The steel absorber/magnet is assumed to be cylindrical with a diameter of 20 mm and a length of 80 mm, with an equivalent density of 7850kg/m^3 and a modulus of elasticity of 200GPa. The mass, M_d hence becomes 0.190 kg. To house this absorber/magnet, the hollow cavity within the copper section of the boring bar is assumed to be of a length of 100 mm.

For the case of a boring bar integrated with only a steel absorber with a mass of 0.190 kg, K_d and C_d were identified by solving Eq. (35) to be 1.485×10^6 N/m and 211.5 N-s/m, respectively. These parameters may be treated as optimally tuned. The dynamics characterized by the real part of the frequency response function at the free cutting end for such a boring bar with an optimally tuned absorber is shown in Fig. 5. To contextualize the improvement in the dynamics with dampers, Fig. 5 also shows the response of a solid boring bar made of steel. And as is evident, the minimum of the real part of the FRF for the optimally tuned absorber is ~76.6 times dynamically stiffer. And, since the chatter-free depth of cut is inversely proportional to the minimum of the real part of the FRF, a corresponding improvement in the cutting performance is expected.

However, since it may not be always possible to optimally tune absorber parameters due to changing loading and boundary conditions, the absorber's stiffness and damping may take on values other than optimal, i.e., it will become detuned. It is also possible that the absorber's support

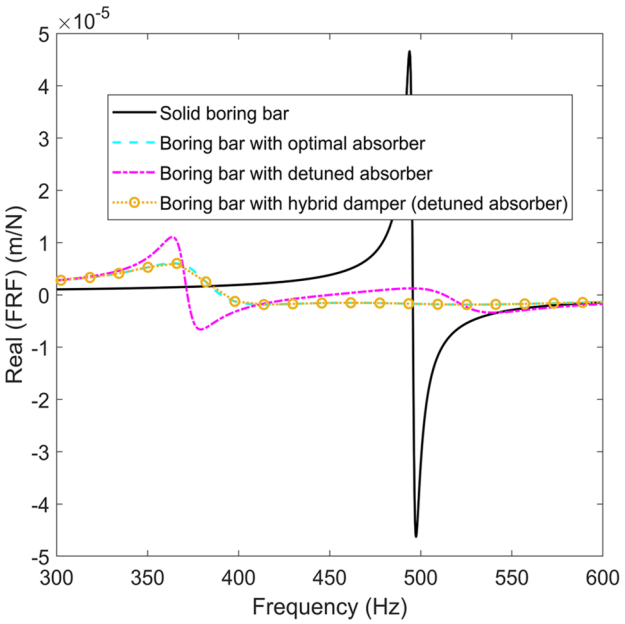

Fig. 5 Real part of the FRF for different configurations of the boring bar

stiffness and damping parameters remain the same, i.e., at their originally set parameters, and the primary system's dynamics change. In this case, also the absorber will become detuned, since, if it was tuned correctly, it would likely have been tuned to match the original dynamics of the primary system. In either case, the system is detuned. And since the aim of this paper is to investigate the influence of an eddy current damper working in conjunction with such a potentially detuned absorber, instead of assuming that the primary system's dynamics change to make the absorber detuned, we instead assume that the primary system's dynamics remain unchanged and that the absorber's support stiffness and damping change.

If, for example, the absorber's mass remained 0.190 kg, and its support stiffness and damping were taken to be 1.478×10^6 N/m and 62 N-s/m, respectively, i.e., parameters other than optimal, then the response of the boring bar with such a detuned absorber would become as shown in Fig. 5. And as is evident, the boring bar with a detuned absorber does not fare as well as the boring bar with an optimally tuned absorber.

Now, if the hybrid damper was to work in conjunction with such a detuned absorber since the overall damping is a superposition of that from the eddy current damper (149.14 N-s/m) and that from the absorber's support, the total damping would become 211 N-s/m, i.e., the total damping can at most take on a value that is optimal for a properly (optimally) tuned absorber. And, for such a case, i.e., the case of a hybrid damper, the response shown in Fig. 5 is significantly stiffer than the response of a boring bar with a

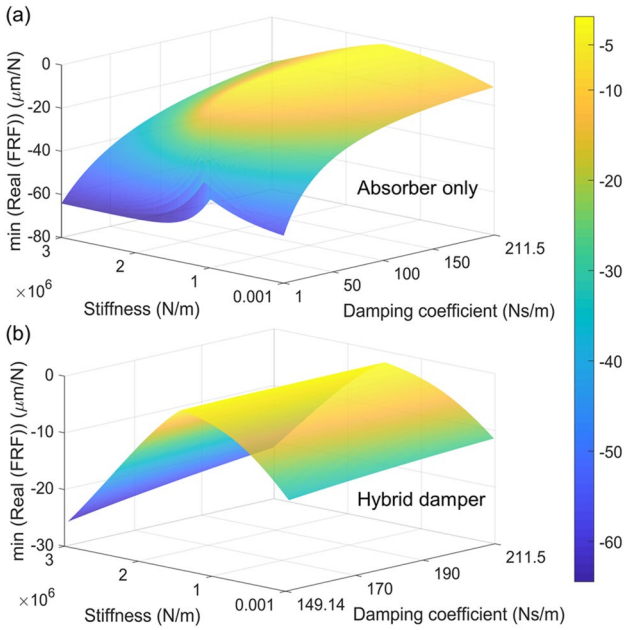

Fig. 6 Minimum of the real part of the FRF shown changing with varying support parameters for: (**a**) a boring bar with a potentially detuned absorber, (**b**) a boring bar with a hybrid damper

detuned absorber, and as dynamically stiff as the response of a separate system with only an optimally tuned absorber. This suggests that the eddy current damper does indeed play a compensatory role and improves the damping performance of a boring bar with a sub-optimally tuned absorber.

If detuned, the absorber's/magnet's support stiffness and damping could take on many other different values than those reported above. These values cannot be known a priori. The stiffness and damping parameters of the absorber are hence varied over a range to evaluate what role, if any, the eddy current damper plays to improve the overall vibration damping capacity. Figure 6 provides an overview of the performance of a hybrid damper in which the absorber is detuned and compares that response to only an absorber that is potentially detuned by taking on many different parameters that are other than optimal. The performance in Fig. 6 is characterized by the minimum of the negative part of the real part of the FRFs.

Since the optimal damping was found to be 211.5 N-s/m, and since the eddy current damper provides a constant damping of 149.14 N-s/m, damping for the absorber/magnet support in the case of the hybrid damper is varied only between 0 and 62, such as to always keep the total damping below the optimal level, i.e., below 211.5 N-s/m. No such restrictions are imposed on the support stiffness. For the case of the detuned absorber only, the damping can take any value between 0 and the optimal. Hence, Fig. 6 has two scales for the damping axes. The scale for damping of the absorber varies between 0 and 211.5 N-s/m–see Fig. 6(a), and the scale for the hybrid damper varies between 149.14 N-s/m and 211.5 N-s/m as shown in Fig. 6(b).

It is clear from Fig. 6 that for all possible stiffness parameters investigated, when the absorber's damping is less than that of the hybrid damper and when the absorber is not optimally tuned, i.e., when the absorber is detuned, the hybrid damper fares better than the detuned absorber as characterized by the min(Real(FRF)). This confirms that the results shown in Fig. 5 are not one-off, but the hybrid damper can improve damping behavior consistently across many possible detuning scenarios for the absorber. It is further clear from Fig. 6 that when the total damping for both configurations of the boring bar, i.e., for the hybrid damper and for a boring bar with only an absorber, is the same, the min(Real(FRF)) is also the same. This suggests that as the absorber's parameters come closer to the optimal parameters, the response of a boring bar with only an absorber compares with the hybrid damper.

Since the purpose of the damped boring bar is to improve the chatter-free depth of cut, Fig. 7 characterizes how the absolute minimum chatter-free depth of cut (b_{lim}) varies for the same parameter sets shown in Fig. 6. Depths of cuts evaluated and shown in Fig. 7 are based on the minimum of the negative part of the real part of the FRFs shown in Fig. 6, and for assumed cutting of aluminum with a radial cutting coefficient of 580 N/mm^2. Figure 7(a) shows the variation of the chatter-free depth of cut for different parameters of a potentially detuned absorber, and Fig. 7(b) shows how the

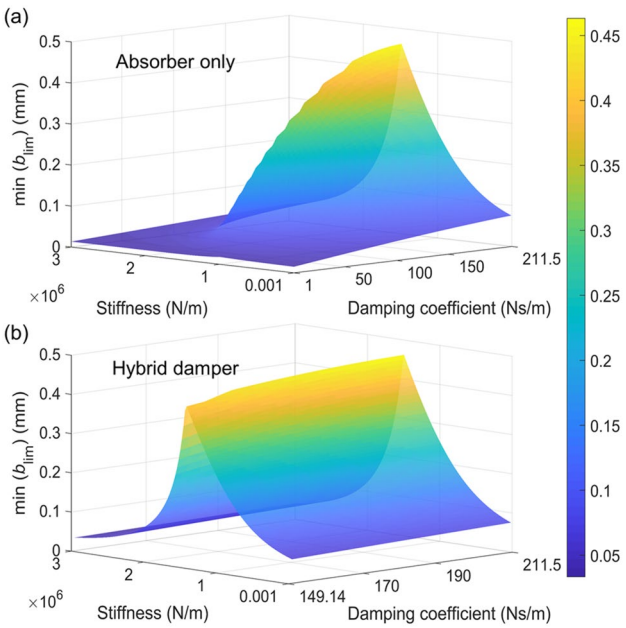

Fig. 7 Minimum chatter-free depth of cut shown changing with varying support parameters for: (**a**) a boring bar with a potentially detuned absorber, (**b**) a boring bar with a hybrid damper

depth of cut changes for different parameters of the hybrid damper.

As is evident from Fig. 7, when the damping of the absorber is less than the damping provided by the hybrid damper, i.e., for the case of a boring bar with a detuned absorber, b_{lim} for the hybrid damper is higher than it is for a boring bar with only a detuned absorber. Since b_{lim} is inversely proportional to the min(Real(FRF)), trends seen in Fig. 7 follow those in Fig. 6. Improvement in the chatter-free depth of cut with a hybrid damper over the case with a detuned absorber is as much as ~ 500%. And, when the absorber is optimally tuned and the hybrid damper takes the maximum possible value of 211.5 N-s/m, the chatter-free depth of cut for both cases is 0.46 mm. And, though this is a whopping 2456% improvement over the case of a solid boring bar without any damper, for which case the b_{lim} is 0.018 mm, since the chatter-free depth of cut for both damped cases was found to be the same, it suggests that if/when the absorber can be optimally tuned, the eddy current damper offers no additional benefit.

Conclusions

This paper demonstrated the workings of a new type of hybrid damper to be integrated within a boring bar to facilitate chatter vibration-free cutting. The hybrid damper consisted of an eddy current damper working in conjunction with a vibration absorber. Analysis for the performance of such a hybrid damper was supported by systematic model-based parametric investigations. We modelled the slender boring bar as an Euler–Bernoulli beam. A permanent magnet was supported in a spring and damper within the boring bar. The supported magnet acted as an absorber and the relative motion between the conductive copper bar and the magnetic field induced eddy currents to hinder the motion of the boring bar. We showed that when the absorber was not optimally tuned, as is often the case with changing boundary conditions and loading scenarios, the eddy current damper plays a compensatory role and makes up for any potential loss of damping due to the absorber being detuned.

Improvement in the chatter-free depth of cut with a hybrid damper over the case with a detuned absorber is as much as ~ 500%. Since our proposed hybrid damping concept consistently results in better vibration damping capacity of the boring bar for many different detuned parameters of the absorber's support stiffness and damping as opposed to a boring bar with just a detuned absorber, our solution is robust to changes. However, when the absorber is optimally tuned and the hybrid damper takes its maximum possible value, the chatter-free depth of cut for both cases was found to be the same, suggesting that if/when the absorber can be optimally tuned, the eddy current damper offers no additional benefit.

Model-based analysis presented herein can inform the design of a prototype for experimental validation, which is necessary, and can form part of future follow-up research. Furthermore, since our models are generalized, they can also be used to guide the integration of hybrid dampers in other tooling systems that suffer from lack of performance due to potentially detuned absorbers. One such case could be milling in which the dynamics of the primary system change with speed and that makes tuning the secondary absorber system difficult.

Acknowledgements This work was supported by the Government of India's Impacting Research Innovation and Technology (IMPRINT) initiative through project number IMPRINT 5509.

Funding Impacting Research Innovation and Technology, 5509, Mohit Law

Declarations

Conflict of interest On behalf of all authors, the corresponding author states that there is no conflict of interest.

References

1. Munoa J, Beudaert X, Dombovari Z, Altintas Y, Budak E, Brecher C (2016) Chatter suppression techniques in the metal cutting. CIRP Ann Manuf Technol 65:785–808. https://doi.org/10.1016/j.cirp.2016.06.004
2. Den Hartog JP (1985) Mechanical vibrations. Dover Publications, New York, USA
3. Asami T, Nishihara O, Baz AM (2002) Analytical solutions to h∞ and h2 optimization of dynamic vibration absorbers attached to damped linear systems. J Vib Acoust Trans ASME 124(2):284–295. https://doi.org/10.1115/1.1456458
4. Sims ND (2007) Vibration absorbers for chatter suppression: a new analytical tuning methodology. J Sound Vib 301:592–607. https://doi.org/10.1016/j.jsv.2006.10.020
5. Tlusty G (2000) Manufacturing equipment and processes. Prentice-Hall, Upper Saddle River
6. Miguélez MH, Rubio L, Loya JA, Fernández-Sáez J (2010) Improvement of chatter stability in boring operations with passive vibration absorbers. Int J Mech Sci 52(10):1376–1384. https://doi.org/10.1016/j.ijmecsci.2010.07.003
7. Rubio L, Loya JA, Miguélez MH, Fernández-Sáez J (2013) Optimization of passive vibration absorbers to reduce chatter in boring. Mech Syst Signal Process 41(1–2):691–704. https://doi.org/10.1016/j.ymssp.2013.07.019
8. Yadav A, Talaviya D, Bansal A, Law M (2020) Design of chatter-resistant damped boring bars using a receptance coupling approach. J Manuf Mater Process. https://doi.org/10.3390/jmmp4020053
9. Rivin EI, Kang H (1992) Enhancement of dynamic stability of cantilever tooling structures. Int J Mach Tools Manuf 32(4):539–561. https://doi.org/10.1016/0890-6955(92)90044-H
10. Akesson H, Smirnova T, Hakansson L (2009) Analysis of dynamic properties of boring bars concerning different clamping

conditions. Mech Syst Signal Process 23:2629–2647. https://doi.org/10.1016/j.ymssp.2009.05.012
11. Altintas Y, Lappin D, Van Zyl D, Östling D (2021) Automatically tuned boring bar system, CIRP Annals, 70(1). ISSN 313–316:0007–8506. https://doi.org/10.1016/j.cirp.2021.04.058
12. Thekkepat AA, Devadula S, Law M (2021) Identifying joint dynamics in bolted cantilevered systems under varying tightening torques and torsional excitations. J Vib Eng Technol. https://doi.org/10.1007/s42417-021-00386-8
13. Patel A, Talaviya D, Law M, Wahi P (2022) Optimally tuning an absorber for a chatter-resistant rotating slender milling tool holder. J Sound Vib 520:116594. https://doi.org/10.1016/j.jsv.2021.116594
14. Yang Y, Wang Y, Liu Q (2019) Design of a milling cutter with large length–diameter ratio based on embedded passive damper, JVC/Journal Vib. Control 25:506–516. https://doi.org/10.1177/1077546318786594
15. Sodano HA, Bae J (2004) Eddy current damping in structures. Shock Vib Dig 36(6):469–478. https://doi.org/10.1177/0583102404048517
16. Paul P, Ingale C, Bhattacharya B (2014) Design of a vibration isolation system using eddy current damper. Proc Inst Mech Eng Part C J Mech Eng Sci 228(4):664–675. https://doi.org/10.1177/2F0954406213489408
17. Bae JS, Kwak MK, Inman DJ (2005) Vibration suppression of a cantilever beam using eddy current damper. J Sound Vib 284(3–5):805–824. https://doi.org/10.1016/j.jsv.2004.07.031
18. Sodano HA, Bae J, Inman DJ, Belvin W (2005) Concept and model of eddy current damper for vibration suppression of a beam. J Sound Vib 288(4–5):1177–1196. https://doi.org/10.1016/j.jsv.2005.01.016
19. Sodano HA, Bae J, Inman DJ, Belvin W (2006) Modeling and application of Eddy current damper for suppression of membrane vibrations. AIAA J 44(3):541–549. https://doi.org/10.2514/1.13024
20. Sodano HA, Bae J, Inman DJ, Belvin W (2006) Improved concept and model of Eddy current damper. J Vib Acoust Trans ASME 128(3):294–302. https://doi.org/10.1115/1.2172256
21. Yang Y, Xu D, Liu Q (2015) Milling vibration attenuation by Eddy current damping. Int J Adv Manuf Technol 81(1–4):445–454. https://doi.org/10.1007/s00170-015-7239-3
22. Chen F, Zhao H, Ding H (2018) Eddy current damper design for vibration suppression in robotic milling process. Proc IEEE Int Conf Robot Autom. https://doi.org/10.1109/ICRA.2018.8460693
23. Singh R, Deiab IM (2019) Non-contact auxiliary fixture for machining stability improvement of thin flexible workpieces using Eddy currents. Int J Interact Des Manuf 13(2):423–440. https://doi.org/10.1007/s12008-018-0495-3
24. Munoa J, Sanz-Calle M, Dombovari Z, Iglesias A, Pena-Barrio J, Stepan G (2020) Tuneable clamping table for chatter avoidance in thin-walled part milling. CIRP Ann 69(1):313–316. https://doi.org/10.1016/j.cirp.2020.04.081
25. Bae JS, Hwang JH, Roh JH, Kim JH, Yi MS, Lim JH (2012) Vibration suppression of a cantilever beam using magnetically tuned-mass-damper. J Sound Vib 331(26):5669–5684. https://doi.org/10.1016/j.jsv.2012.07.020
26. Chen J, Lu G, Li Y, Wang T, Wang W, Song G (2017) Experimental study on robustness of an eddy current-tuned mass damper. Appl Sci 7:895. https://doi.org/10.3390/app7090895
27. Bae JS, Park JS, Hwang JH, Roh JH, Do PB, Kim JH (2018) Vibration suppression of a cantilever plate using magnetically multimode tuned mass dampers. Shock Vib. https://doi.org/10.1155/2018/3463528
28. Beek TA, Pluk KJW, Jansen JW, Lomonova EA (2014) Optimization and measurement of eddy current damping applied in a tuned mass damper. Int Conf Electr Mach. https://doi.org/10.1109/ICELMACH.2014.6960243
29. Berardengo M, Cigada A, Guanziroli F, Manzoni S (2015) Modelling and control of an adaptive tuned mass damper based on shape memory alloys and eddy currents. J Sound Vib 349:18–38. https://doi.org/10.1016/j.jsv.2015.03.036
30. Lian J, Zhao Y, Lian C, Wang H, Dong X, Jiang Q, Zhou H, Jiang J (2018) Application of an eddy current-tuned mass damper to vibration mitigation of offshore wind turbines. Energies. https://doi.org/10.3390/en11123319
31. Bae JS, Hwang JH, Kwag DG, Park J, Inman DJ (2014) Vibration suppression of a large beam structure using tuned mass damper and eddy current damping. Shock Vib. https://doi.org/10.1155/2014/893914
32. Lazoglu I, Atabey F, Altintas Y (2002) Dynamics of boring processes: part III-time domain modeling. Int J Mach Tools Manuf 42:1567–1576. https://doi.org/10.1016/S0890-6955(02)00067-6
33. Hagedorn P, DasGupta A (2007) Vibrations and waves in continuous mechanical systems. John Wiley & Sons Ltd, New Jersey
34. Craik D (1995) Magnetism: principles and applications. John Wiley & Sons Ltd, New Jersy
35. https://radialmagnet.com/. Accessed on 01 Apr 2022
36. Dem'yanov V F, Malozemov V N (1990) Introduction to minimax, courier corporation, USA.